

Relationships between the phase behavior of lattice models of amphiphile mixtures and Griffiths's three-component model

Carmen Varea and Alberto Robledo

División de Estudios de Posgrado, Facultad de Química, Universidad Nacional Autónoma de México, 04510, Distrito Federal, México

(Received 6 August 1985)

We describe various phase equilibrium patterns occurring in multicomponent fluid model mixtures where several amphiphilic species are present. The characterization is based on the existing correspondence of states between the Furman, Dattagupta, and Griffiths (FDG) mixture of three components and a (mean-field) natural extension of the Wheeler-Widom model of bifunctional molecules. The shield region and the multicritical points appearing in the FDG and in the van der Waals binary-fluid models are reproduced in the mixture of amphiphiles through manipulations of composition. The diagrams obtained exhibit three- and four-phase equilibria associated with bulk liquids with structures analogous to those in mixed-micellar and bicontinuous middle-phase microemulsions.

I. INTRODUCTION

Mixtures of surfactants have been found to be more efficient stabilizers of microemulsion systems than single surfactants.^{1,2} The reasons for this may in part originate in the possibility, with two or more species present, of having a multiplicity of phase interface and micellar structures. It has been suggested³ that cosurfactants play an important role in producing an enhanced flexibility in the microscopic interface between the oil- and the water-filled regions. This flexibility permits the existence of transparent fluid phases of low viscosity among the more common regularly organized liquid-crystalline phases.³ Also, a salient feature of microemulsion systems is their unusual phase equilibria, where progressions from three to four liquid phases, two of which may be microemulsion phases, can be generated with changing temperature or composition.⁴⁻⁶ Most of these observations correspond to commercial formulations for which surfactant mixtures, rather than pure entities, are commonly used.⁶

Here we describe some phase diagrams pertaining to multicomponent lattice models of bifunctional molecules, several of which are given amphiphilic character. We shall also see that the bulk phases allow for mixed-micellar and bicontinuous configurations with various surfactant-cosurfactant film geometries. These appear as useful simplified versions of those occurring in surfactant solutions and microemulsions.

The model mixture is a straightforward extension, to six components in a five-dimensional field space, of the Widom-Wheeler (WW1) lattice mixture of three bifunctional species.⁷ The extended version (which we shall refer to as the WW2 model), when described in a mean-field approximation, maps onto the Furman, Dattagupta, and Griffiths (FDG) three-component model.⁸ The WW2 model becomes therefore another way of interpreting the FDG model, which may be thought of also as (mean-field approximations of) the spin-1 Ising magnet, a regular mixture of three components, and a model mixture of two compressible fluids.⁸ We take advantage of the above-

mentioned mapping to translate the known behavior of the FDG model into bifunctional mixture language. The entire, five-dimensional-parameter, global phase diagram of the FDG model has been discussed in detail previously.⁸

We briefly recall the main properties of the WW1 model. Wheeler and Widom⁷ described a model mixture in a lattice that abstracts some of the essential features of a ternary system composed of water, oil and surfactant. The WW1 model is isomorphous to the Ising spin- $\frac{1}{2}$ model in the same lattice, and displays as corresponding states both ferromagnetic and antiferromagnetic behavior. The binodal curve and plait point of the mixture are images of the spontaneous magnetization and Curie point of the ferromagnet, respectively. At a high concentration of surfactant, antiferromagneticlike ordering appears. The model is composed of bifunctional molecules AA ($\circ-\circ$), BB ($\bullet-\bullet$), and AB ($\circ-\bullet$), and it is constructed by: (i) confining the molecules to the bonds of a regular (in our case, three-dimensional) lattice; (ii) letting only A atoms or only B atoms meet at any lattice site (the A ends of one molecule and the B ends of another exclude each other); and (iii) filling every bond of the lattice with one, and only one, molecule. Since for all the allowed configurations every site can be identified as either an A or a B site, the equivalence to the Ising model follows. The complete transcription to fluid-mixture language, the model's phase diagram, and the mean-field description of the interface between coexisting phases is given in Ref. 7. Because every bond in the lattice is filled by one molecule, the chemical potentials μ_{AA} , μ_{BB} , and μ_{AB} of the three species are infinite, but the difference of any pair is in general finite. In particular, when the mixture and the magnet are set at the same temperature, the chemical potential differences are related to the Ising coupling J by⁷

$$\tilde{\mu}_{AB} \equiv \mu_{AB} - \frac{1}{2}(\mu_{AA} + \mu_{BB}) = -2J. \quad (1)$$

We call $\tilde{\mu}_{AB}$ the (relevant) surfactant chemical potential. Since the potential energy of every allowable configura-

tion always vanishes, the mixture's temperature does not play a relevant role. In Fig. 1 we show the model's phase diagram. The behavior of the mixture is easily understood when correspondence of states is at fixed temperature. Then, from Eq. (1) we observe that addition of surfactant AB to a mixture with a given AA to BB ratio (say $\mu_{AA} - \mu_{BB}$ fixed) implies a reduction of the Ising coupling constant at the same temperature. $J \rightarrow \infty$ at the base line $x_{AB}=0$, J changes sign at a locus of intermediate compositions $x_{AB}^2/x_{AA}x_{BB}=4$, $\tilde{\mu}_{AB}=0$,⁷ when the spins are uncoupled, and finally $J \rightarrow -\infty$ for pure surfactant, $x_{AB}=1$. The lower curve in Fig. 1 is the coexistence curve of AA -rich and BB -rich phases, the (horizontal) tie lines terminate at the critical solution point β . The dashed line separates the region of compositions where the mixture is analogous to a ferromagnet from that in which it is analogous to an antiferromagnet. The upper curve demarcates the onset of antiferromagnetic (sublattice) order.

The WW2 model is obtained by incorporating the three new species CC ($\odot-\odot$), AC ($\circ-\odot$), and BC ($\bullet-\odot$) into the lattice with the same bond-filling rules as before. Every site can be labeled as an A , B , or C site and the model is equivalent to a three-component mixture where atoms occupy sites. Some examples of allowed configurations are illustrated in Fig. 2. Figure 2(b) represents a mixed micelle embedded in a sea of AA molecules. Figure 2(c) shows two alternative surfactant film structures separating BB - and AA -filled regions. The three species AC , CC , and BC can be considered cosurfactants, and, as we shall see, they are only required in small proportions to generate interesting phase progressions. Alternatively, the CC species can be labeled "vacuum" and the three molecules AB , AC , and BC may represent the same amphiphilic species, with the label indicating when it is located between the two immiscible solvents AA and BB , or when at a liquid-gas interface. In both cases the model exhibits

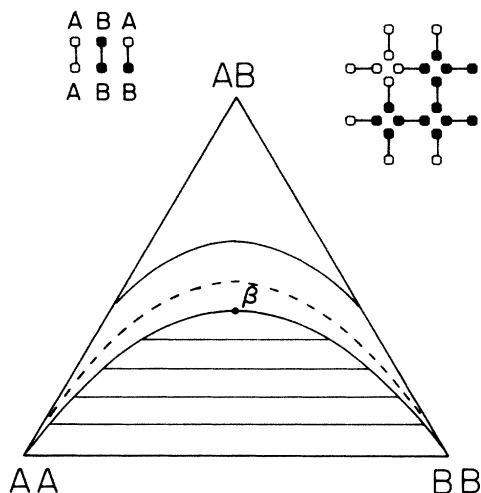


FIG. 1. Phase diagram for the WW1 model of bifunctional molecules AA , BB , and AB . The lower curve is the coexistence curve with horizontal tie lines, the dashed curve represents independent spins in the Ising analogue, and the upper curve sublattice ordering.

three-liquid-phase equilibria and critical end points, which are features absent in the WW1 version.

In the next section we show the equivalence between the partition functions of the WW2 model and the three-component mixture. In Sec. III we transcribe some of the phase diagrams of the FDG model into WW2 language for the full six-component case. In Sec. IV we describe the particular three-component version when CC represents vacuum and there is only one kind of amphiphile. We summarize our results in the final section, Sec. V.

II. SIX-COMPONENT MODEL

Let N_{AA} , N_{BB} , N_{AB} , N_{CC} , N_{AC} , and N_{BC} be the numbers of each bifunctional species in the mixture, M the total number of sites in the lattice, and Z its coordination number. Also, let N_A , N_B , and N_C be the numbers of sites identified as A , B , or C sites, respectively. Because every bond in the lattice is filled and every site can be unambiguously labeled A , B , or C , the following relations are satisfied:

$$2N_{AA} + N_{AB} + N_{AC} = ZN_A, \quad (2a)$$

$$2N_{BB} + N_{AB} + N_{BC} = ZN_B, \quad (2b)$$

$$2N_{CC} + N_{AC} + N_{BC} = ZN_C, \quad (2c)$$

and

$$N_A + N_B + N_C = M. \quad (2d)$$

We denote by $Q(\circ, \bullet, \odot)$ the number of distinguishable ways of placing the given N_{AA} , N_{BB} , N_{CC} , N_{AB} , N_{AC} , and N_{BC} molecules on the lattice bonds. And we formally write the grand partition function of the WW2 model as

$$\Xi(T, \{\mu_{ij}\}) = \sum' Q(\circ, \bullet, \odot) \exp \left[-\beta \sum_{i,j=A,B,C} \mu_{ij} N_{ij} \right], \quad (3)$$

where $\beta = 1/kT$, k is Boltzmann's constant, and T is the absolute temperature; the summation \sum' is over all values

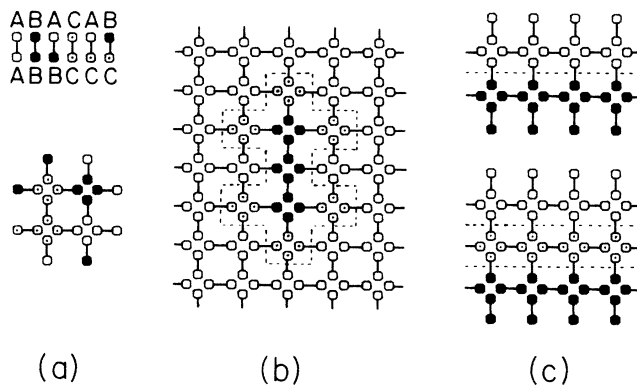


Fig. 2. Six bifunctional molecules of the WW2 model on the bonds of a lattice. (a) Only ends of the same kind meet at any lattice site. (b) Mixed micelle in an AA -filled region. (c) Two alternative surfactant film structures separating AA - and BB -filled regions.

of the N_{ij} such that $\sum_{ij} N_{ij} = \frac{1}{2} ZM$, and the μ_{ij} are the chemical potentials. With the employment of Eqs. (2), Eq. (3) can be transformed into

$$\begin{aligned} \Xi(T, \mu_A, \mu_B; a, b, c) &= \sum' Q(\circ, \bullet, \odot) \exp[\beta(aN_{BC} + bN_{AC} + cN_{AB})] \\ &\quad \times \exp[-\beta(\mu_A N_A + \mu_B N_B)] \exp\left[-\beta \frac{Z}{2} \mu_{CC} M\right], \end{aligned} \quad (4)$$

where

$$-a = \tilde{\mu}_{BC} \equiv \mu_{BC} - \frac{1}{2}(\mu_{BB} + \mu_{CC}), \quad (5a)$$

$$-b = \tilde{\mu}_{AC} \equiv \mu_{AC} - \frac{1}{2}(\mu_{AA} + \mu_{CC}), \quad (5b)$$

$$-c = \tilde{\mu}_{AB} \equiv \mu_{AB} - \frac{1}{2}(\mu_{AA} + \mu_{BB}), \quad (5c)$$

$$\mu_A = \frac{Z}{2}(\mu_{AA} - \mu_{CC}), \quad (6a)$$

and

$$\mu_B = \frac{Z}{2}(\mu_{BB} - \mu_{CC}). \quad (6b)$$

Since $Q(\circ, \bullet, \odot)$ is also the number of different ways of filling the lattice sites with N_A , N_B , and N_C atoms of types A , B , and C , respectively, Eq. (4) represents the partition function of a three-component mixture of these atoms. The parameters a , b , and c represent pair interactions and μ_A and μ_B are the chemical potentials of species A and B . The last exponential factor in Eq. (4) collects the divergence of the chemical potentials μ_{ij} of the close-packed lattice. Equations (5) and (6) state the equivalence between the (five independent) fields of the WW2 model and those of the three-component mixture. To obtain the thermodynamic potential that corresponds to the FDG model we adopt the mean-field approximations $N_{BC} = (ZM/2)N_B N_C$, $N_{AC} = (ZM/2)N_A N_C$, and $N_{AB} = (ZM/2)N_A N_B$ and thus simplify the relationship between the bond and the site numbers. It is also necessary to make explicit the combinatorial expression for Q ,

$$Q(\circ, \bullet, \odot) = \frac{M!}{N_A! N_B! N_C!}. \quad (7)$$

It follows that the grand potential $\Omega = -kT \ln \Xi$ acquires the form (for large M)

$$\Omega = G - \mu_A M n_A - \mu_B M n_B, \quad (8)$$

where

$$\begin{aligned} G = M \left[kT(n_A \ln n_A + n_B \ln n_B + n_C \ln n_C) \right. \\ \left. + \frac{ZM}{2}(a n_B n_C + b n_A n_C + c n_A n_B) \right], \end{aligned} \quad (9)$$

where $n_A = N_A/M$, $n_B = N_B/M$, and $n_C = N_C/M$. Equations (8) and (9) coincide with the phenomenological definition of the FDG model.

Since multiplication of Eq. (8) by a positive factor has no influence on phase equilibrium, Furman, Dattagupta,

and Griffiths⁸ found it convenient to normalize the interaction parameters a , b , and c in their description of phase diagrams. In our notation they adopted the condition $(ZM/2)(|a| + |b| + |c|) = 1$. Also, they chose as the five independent field variables $\bar{a} = a/MkT$, $\bar{b} = b/MkT$, $\bar{c} = c/MkT$, μ_A , and μ_B , and from the given values of \bar{a} , \bar{b} , and \bar{c} , a measure of temperature was obtained, since $ZM^2 kT/2 = (|\bar{a}| + |\bar{b}| + |\bar{c}|)^{-1}$. Here we shall be interested, as with the WW1 case, in establishing a correspondence between states when the bond and the site mixtures are set at the same temperature. This correspondence is expressed by Eqs. (5). We observe, as before, that addition of, say, species BC to the mixture implies a reduction of the image interaction parameter a , and similarly with AC and AB . $a \rightarrow \infty$ when $x_{BC} = 0$ and $a = 0$ at the intermediate compositions (fixed by the ratios of the other components) when $\tilde{\mu}_{BC}$ vanishes. Beyond this compositions there appear "antiferromagnetic" analogs, as in the WW1 model. We shall not discuss them here as they were also not included in Ref. 8.

To make direct use of the global phase diagram of the FDG model we define

$$\hat{\mu}_{BC} \equiv \tilde{\mu}_{BC} / |\mu|, \quad (10a)$$

$$\hat{\mu}_{AC} \equiv \tilde{\mu}_{AC} / |\mu|, \quad (10b)$$

and

$$\hat{\mu}_{AB} \equiv \tilde{\mu}_{AB} / |\mu|, \quad (10c)$$

where $|\mu| \equiv |\tilde{\mu}_{BC}| + |\tilde{\mu}_{AC}| + |\tilde{\mu}_{AB}|$. These parameters are normalized, $|\hat{\mu}_{BC}| + |\hat{\mu}_{AC}| + |\hat{\mu}_{AB}| = 1$, and $|\mu|$ plays the role of the inverse temperature in Ref. 8.

Relation with the van der Waals (vdW) model. When one of the three (site) species in the FDG model is labeled "vacuum," a lattice version of the van der Waals binary mixture is obtained. The vdW mixture has been studied extensively by Scott and van Konynenburg,⁹ and the similarities between the global phase diagrams of the vdW and the FDG models have been discussed before.¹⁰ The correspondence between the vdW mixture field variables and those of the WW2 model is as follows:

$$\alpha_{11} = -\frac{Z}{2}[\mu_{AC} - \frac{1}{2}(\mu_{AA} + \mu_{CC})], \quad (11a)$$

$$\alpha_{22} = -\frac{Z}{2}[\mu_{BC} - \frac{1}{2}(\mu_{BB} + \mu_{CC})], \quad (11b)$$

$$\alpha_{12} = -\frac{Z}{2}(\mu_{AB} + \mu_{CC} - \mu_{AC} - \mu_{BC}), \quad (11c)$$

$$\mu_1 = -\frac{Z}{2}(\mu_{AC} - \mu_{CC}), \quad (11d)$$

and

$$\mu_2 = -\frac{Z}{2}(\mu_{BC} - \mu_{CC}), \quad (11e)$$

where the α_{ij} and the μ_i are, respectively, the interaction parameters and the chemical potentials of the two species 1 and 2.

III. PHASE DIAGRAMS

Because the WW2 model (in the mean-field approximation) is one of several realizations of the FDG model, it displays its full five-dimensional phase diagram (including sublattice-ordered "antiferromagnetic" phases not discussed in Ref. 8). The most interesting property of the WW2 model is that all field variables are combinations of chemical potentials, and, therefore, important features in the phase diagram can be "tuned in" only by means of alterations in composition. Other realizations of the FDG model, like the three- (site) component mixture, require the alteration of the "nature" of the system in order to observe some phase progressions. In all of these cases, a system phase diagram corresponds to a section of the full diagram obtained by keeping a , b , and c fixed. We shall not produce here a systematic translation of the full phase behavior, which can be carried out in a straightforward way through the employment of Eqs. (5), (6), and (10). Instead, we describe two particular cases where the phase behavior develops naturally with change in global composition in the WW2 model. These are the so-called symmetrical section⁸ and another section obtained when one of the three interaction parameters is fixed. There are three equivalent sections of each kind since they are transformed into each other when the permutation symmetry of the model is taken into account. [Any permutation of a , b , and c , accompanied by the corresponding permutation of n_A , n_B , and n_C leaves G in Eq. (9) unchanged.] We shall think of AA as representing "oil," BB "water," AB the "main surfactant," and AC , BC , and CC the "cosurfactants."

A. Symmetrical section

From Eqs. (5) and (6) we note that the symmetrical section $a = b$ under the additional restriction that $\mu_A = \mu_B$ can be obtained when the oil-to-water ratio x_{AA}/x_{BB} is fixed to be unity, and when equal amounts of the cosurfactants AC and BC are always present. In Fig. 3 we show the portion of the symmetrical section $\tilde{\mu}_{BC} = \tilde{\mu}_{AC}$ with $\tilde{\mu}_{AB}$, $\tilde{\mu}_{BC}$, and $\tilde{\mu}_{AC}$ negative (a , b , and c positive, "the principal energy triangle"⁸) projected on the $|\mu|^{-1}$ -versus- $\hat{\mu}_{AB}$ plane. Only the main features of the section, which happen to appear precisely when $\mu_A = \mu_B$, are marked in the figure. The desired value of μ_A can be obtained by additions or removals of the species CC . We follow a similar notation for phase coexistence and critical boundaries as in Ref. 8. Thus, α^2 represents two coexisting phases and β denotes a conventional critical point where the two phases coalesce. Likewise, three-phase states α^3 terminate at a critical end point $\alpha\beta$ or at a tricritical point γ . Four-phase states α^4 may appear bounded by critical points coexisting with two phases $\alpha^2\beta$, by a double critical point β^2 , by a tricritical end point $\alpha\gamma$, or by a fourth-order critical point δ .

The symmetrical section contains two different regions of four-phase coexistence. The first one appears at low concentrations of AB and also of AC and BC ($\hat{\mu}_{AB} \sim -1$ and $|\mu|^{-1} \sim 0$), when there are not sufficient mixed bifunctional bonds to "dissolve" the majority AA , BB , and, probably to a lesser extent, CC bonds. These four-phase

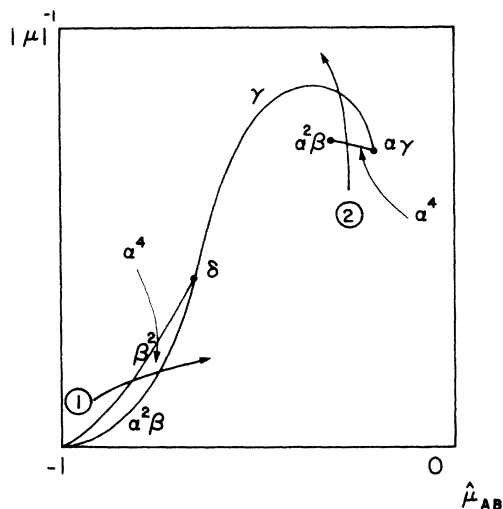


FIG. 3. Projection of the symmetrical section $\tilde{\mu}_{BC} = \tilde{\mu}_{AC}$ of the full phase diagram on the $|\mu|^{-1}$ -vs- $\hat{\mu}_{AB}$ plane. This figure is essentially that of FDG (Ref. 8) Fig. 8. The notation for phase coexistence and critical boundaries is explained in the text. The arrows labeled 1 and 2 indicate field variations corresponding to the phase progressions shown in Figs. 4 and 5, respectively.

states are bounded by two locuses of β^2 and $\alpha^2\beta$ points, which merge at a δ point at higher surfactant concentration. Addition of the main surfactant AB to the mixture, produces the phase progression shown in Fig. 4, where the insets show the appearance of mixtures of composition P (poor in the cosurfactant CC). The trajectory followed in $|\mu|^{-1}$ -versus- $\hat{\mu}_{AB}$ space is represented by the arrow labeled 1 in Fig. 3. Essentially the same phase progression, demarcated by β^2 and $\alpha^2\beta$ states, was obtained by Talmon and Prager¹¹ in a phenomenological study of a microemulsion system. The main trait of their model is a random oil-water "bicontinuous" (or multiply connected) geometry where the surfactant molecules are confined to the interfacial film that separates oil- from water-filled regions.^{11,12,13} The transformation from two- to four- and then to three-phase coexistence was observed by increasing the spatial extent of the surfactant film that separates equal amounts of oil and water. As in our case, in the original Talmon-Prager model there is a built-in symmetry between the oil and water components. This symmetry is responsible, in their three-component model, for the apparent violation of the phase rule by the four-phase states. Whereas in the WW2 model, the cosurfactants provide extra degrees of freedom that permit variation in the concentration of surfactant AB at AA/BB microscopic interfacial regions without alteration of its total amount in the sample. This feature is incorporated in the Talmon-Prager model,¹¹ and its extensions,^{12,13} through a size parameter that determines the scale of the microemulsion structure.

The fourth-order point δ in Fig. 3 is also the common end of a line of symmetrical tricritical points that span an interval of surfactant AB compositions. At the other end of this interval the line terminates at an $\alpha\gamma$ point, which

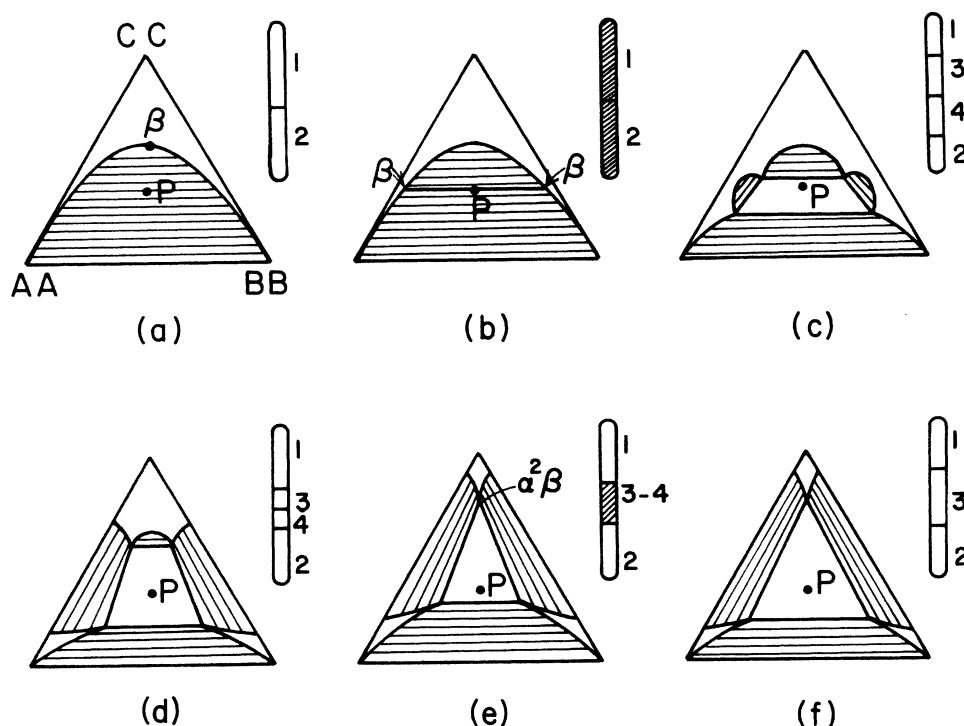


FIG. 4. Phase progression generated by addition of the main surfactant AB to a mixture with equal amounts of AA and BB and also of AC and BC . The insets show the physical appearance of mixtures of composition P , which lies on the tie line between two critical points.

in turn bounds the second set of four-phase states together with an $\alpha^2\beta$ point. This other set of α^4 points forms part of the shield region and extends out of the symmetrical section, where other $\alpha^2\beta$ and $\alpha\gamma$ points demarcate its limits.⁸ Addition of AC and BC (which we have chosen to keep always in equal quantities) to the mixture yields the phase progression shown in Fig. 5. Again, the insets show the physical appearance of mixtures of composition P . The trajectory followed in $|\mu|^{-1}$ -versus- $\hat{\mu}_{AB}$ space is shown by the arrow labeled 2 in Fig. 3.

B. Section with $\tilde{\mu}_{AB} = -c$ fixed

Another interesting section of the phase diagram is obtained when $\tilde{\mu}_{AB}$ is fixed. In Fig. 6 we show a portion of this section when the relevant chemical potentials $\tilde{\mu}_{AB}$, $\tilde{\mu}_{BC}$, and $\tilde{\mu}_{AC}$ are negative (i.e., when species AB , AC , and BC appear in relatively small quantities). The figure is a projection on the $|\mu|^{-1}$ -versus- $\hat{\mu}_{BC}$ plane in the case when $\tilde{\mu}_{AB}$ is sufficiently negative (or $\hat{\mu}_{AB}$ sufficiently close to -1) so that the section passes through the regions in the "principal energy triangle" labeled $P_{\alpha\beta}$, $P_{\alpha\gamma}$, and P_γ in Ref. 8. Strictly speaking this section is spanned by fixing the field $\tilde{\mu}_{AB}$ while varying the other fields $\tilde{\mu}_{BC}$ and $\tilde{\mu}_{AC}$ (at fixed $|\mu|$, when $\tilde{\mu}_{BC}$ is increased, $\tilde{\mu}_{AC}$ diminishes by the same amount). In practice, a first approximation in obtaining this section, and one which does not affect our arguments in principle, would be to fix the composition x_{AB} , while varying the ratios of other species. Specifically, from Eqs. (5) we observe that a simple prescription would be to vary the cosurfactant ratio

x_{BC}/x_{AC} while fixing the oil-to-water ratio x_{AA}/x_{BB} and the quantities present of the main surfactant AB and the cosurfactant CC . As before, the amount of CC is an extra degree of freedom with which μ_A and μ_B can be "tuned in" to observe some desired features.

Figure 6 is composed of three lines of critical end points joined by a tricritical point γ and a double critical point β^2 . They are also bounded by one $\alpha^2\beta$ point. The locus of the $\alpha\beta$ points does not intersect itself in the full phase diagram although it appears to do so in the $|\mu|^{-1}$ -versus- $\hat{\mu}_{BC}$ projection. The arrow labeled 1 in Fig. 6 corresponds to the phase progression shown in Fig. 7. These phase diagrams show the evolution of three-phase states bounded by two different critical end points. In Fig. 7(a) it is the phase almost pure in oil AA and another one, the "middle" phase, rich in AB and with relatively balanced proportions of AA and BB , that become critical. In Fig. 7(c) the three-phase triangle has become symmetrical, and in Fig. 7(e) the phase rich in water BB and the middle phase become critical. This evolution of three-phase states is very similar to that observed in real microemulsion systems consisting of oil, brine, surfactant and cosurfactant,^{4,5} and in recent phenomenological studies of the same type of systems.¹³ There, the relative amounts of the mixture components are kept fixed while the salinity of the brine is varied. In our case, the variation of the cosurfactant ratio x_{BC}/x_{AC} is seen to play an equivalent role. This equivalence is not surprising since variation of brine salinity has been related to changes in the surfactant film curvature (the so-called Bancroft parameter).^{12,13,14} In the WW2 model a surfactant film that separates AA from BB regions of the kind shown at the

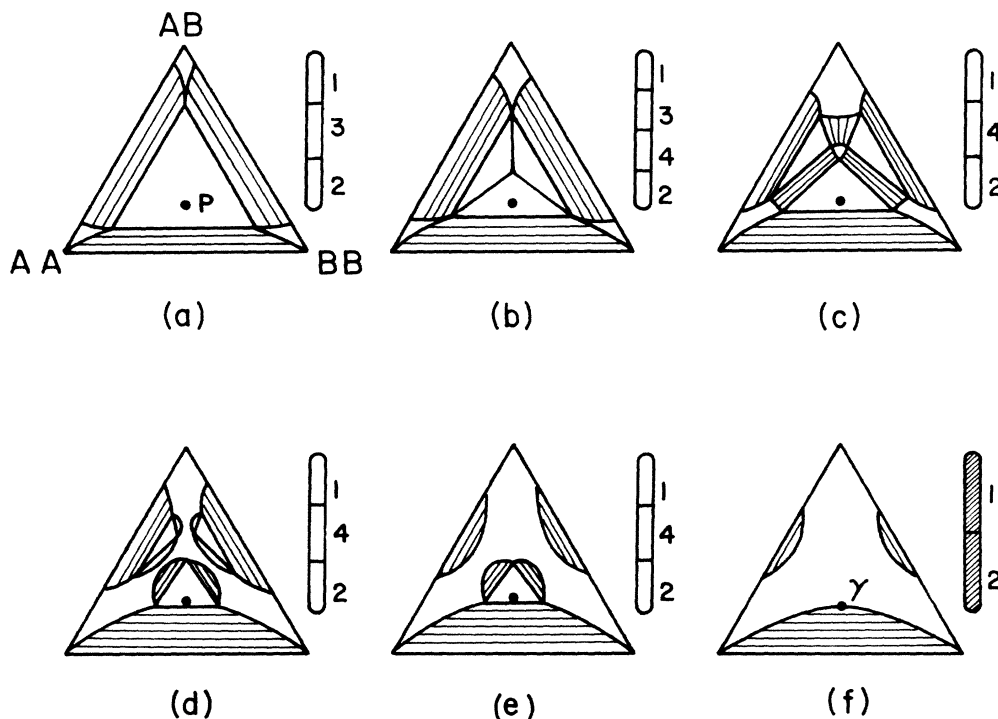


FIG. 5. Phase progression generated by addition of the cosurfactants AC and BC (present in equal quantities) to a mixture with fixed amounts of the other species. The AA/BB ratio is unity.

bottom of Fig. 2(c) has average zero curvature when the amounts of AC and BC that constitute it are equal. Changes in the film curvature can be achieved through variation of the ratio x_{BC}/x_{AC} .

Of course, given the five degrees of freedom of the WW2 model, there are other ways of changing composition that generate essentially the same phase behavior as illustrated in Fig. 7. Moreover, there are several regions of the full phase diagram, some of which lie outside the

principal energy triangle, that exhibit three-phase points bounded by two different critical end points.⁸ In all of these regions there are sections that contain phase progressions qualitatively similar to that of Fig. 7. At lower values of $|\mu|^{-1}$ (smaller overall amounts of AC and BC , or larger quantities of CC), when $|\mu|^{-1}$ lies between those values at which β^2 and $\alpha^2\beta$ occur, we have more complex phase progressions (represented by the arrow labeled 2 in Fig. 6) involving four-phase states and two different three-phase lines. This is shown in Fig. 8.

IV. COMPRESSIBLE THREE-COMPONENT MODEL

The six components of the WW2 model can be reduced to only three if the CC species is labeled vacuum and the three amphiphilic species are considered to be only one. An AB bond indicates a molecule of amphiphile joining AA - and BB -filled regions, or forming empty micelles in one or the other immiscible liquids. An AC or a BC bond represent the same molecule of amphiphile but now located at liquid-gas interfacial regions, or constituting micellar, or "aerosol," particles in the gas phase. The species CC may also be thought of as a thermodynamically inert gas, like air, poorly soluble in either pure immiscible liquid. In this case, the amphiphile increases not only the mutual solubility of the liquid but also that of the gas in the liquids.

The (mean-field) thermodynamic properties of this model can be obtained from the known behavior of the FDG model by identifying the region occupied in the full phase diagram. The model requires that $\mu_{CC}=0$ and that $\mu_{AB}=\mu_{BC}=\mu_{AC}$, so that there are left three degrees of freedom out of the original five in the WW2 model.

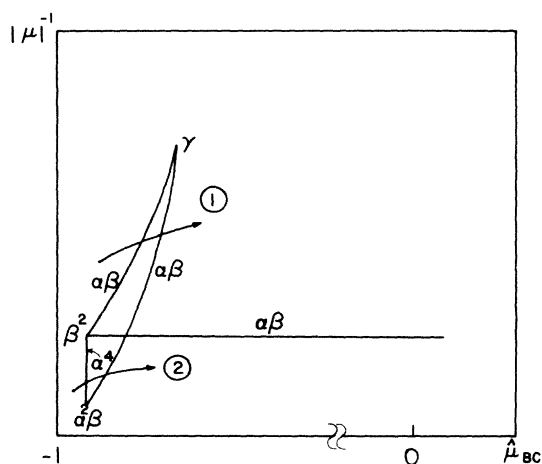


FIG. 6. Projection of the section with $\tilde{\mu}_{AB}$ fixed of the full phase diagram on the $|\mu|^{-1}$ -vs- $\tilde{\mu}_{BC}$ plane. The arrows labeled 1 and 2 indicate field variations corresponding to the phase progressions shown in Figs. 7 and 8, respectively.

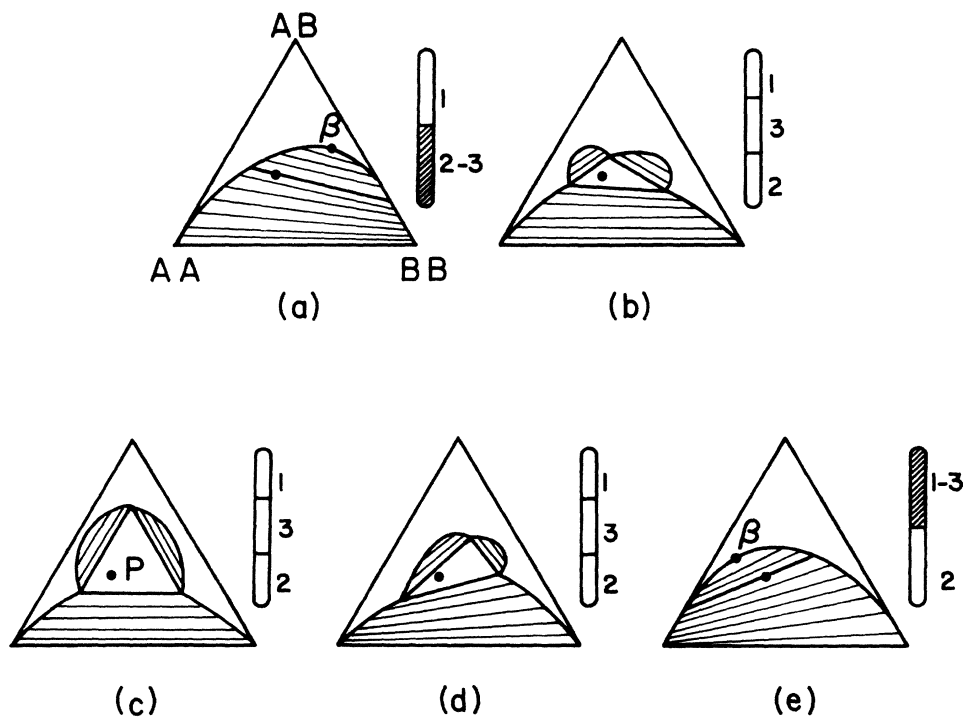


FIG. 7. Phase progression obtained by increasing the BC/AC ratio of cosurfactants to a mixture where the ratio AA/BB and also those quantities present of AB and CC are fixed. See arrow labeled 1 in Fig. 6.

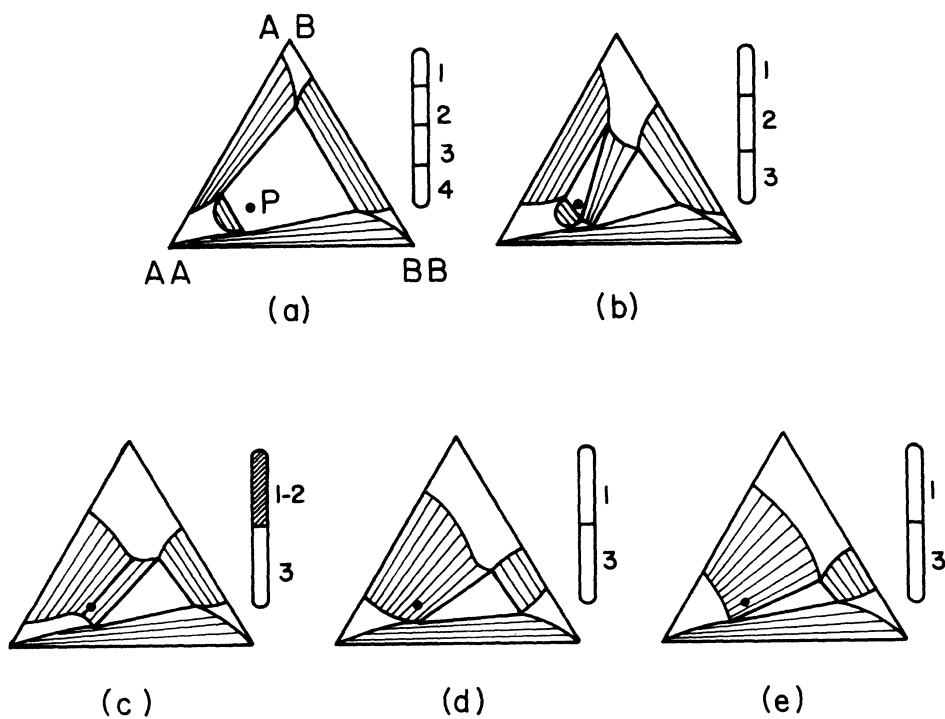


FIG. 8. Phase progression obtained by increasing the BC/AC ratio of cosurfactants to a mixture with conditions similar to those of Fig. 1, but here the value of $|\mu|^{-1}$ is smaller. See arrow labeled 2 in Fig. 6.

These may be represented directly by the fields μ_{AA} , μ_{BB} , and μ_{AB} , which are now in general finite, as is the pressure $p = -\Omega/M$. From Eqs. (5) and (6) we have that

$$a = -(\mu_{AB} - \frac{1}{2}\mu_{BB}), \quad (12a)$$

$$b = -(\mu_{AB} - \frac{1}{2}\mu_{AA}), \quad (12b)$$

$$c = -[\mu_{AB} - \frac{1}{2}(\mu_{AA} + \mu_{BB})], \quad (12c)$$

$$\mu_A = \frac{Z}{2}\mu_{AA} = Z(a - c), \quad (13a)$$

and

$$\mu_B = \frac{Z}{2}\mu_{BB} = Z(b - c). \quad (13b)$$

We observe that the chemical potentials μ_A and μ_B are determined by the current values of the interaction parameters a , b , and c . Hence the phase diagram of our three-component version is built up by selecting, according to Eqs. (13), one thermodynamic state from each system phase diagram of the FDG model.

It is interesting to note that the compressible model when viewed as a special case of the WW2 model preserves the rules to fill the bonds (i.e., only like ends of bifunctional molecules meet at a given site). However, when the allowed configurations of the three species in this compressible version are examined in terms of the WW1 model it is found, in contradiction to the WW1 model, that several molecules of the amphiphile AB may meet at a given site through both like and unlike ends. Only the species AA and BB preserve the original rules. Thus, the fully compressed pure AB substance does not exhibit sublattice ordering.

We performed calculations for the phase diagrams corresponding to the symmetrical section, that is, for the case when the oil-to-water ratio is unity. We found when increasing the pressure that the path of states followed essentially that described by the arrow labeled 2 in Fig. 3. The phase progression when the sample is compressed is qualitatively identical to that shown in Fig. 5. Increasing pressure incorporates additional quantities of surfactant at oil-water interfacial regions that were formerly at gas-liquid interfaces, and as a consequence, the two immiscible substances AA and BB are more efficiently solubilized. It is worth noticing that this process is assisted by the appearance of an intermediate four-phase state that connects the low-pressure three-phase states (a gas and two liquids, one rich in AA and the other in BB) with the high-pressure three-phase states (three liquids, two as before and the third a "middle"-phase-type microemulsion). The mechanism is that provided by the nature of the shield region of the FDG model.

V. SUMMARY AND DISCUSSION

The original Wheeler and Widom mapping of a ternary fluid onto an Ising model (lattice gas, or binary alloy) was intended to mimic only certain broad features of mixtures of bifunctional molecules. In particular, near the Ising critical point the artificialities of the model become irrelevant and correct predictions can be obtained for the behavior of the mixtures' consolute point. Further, the

model captures the microscopic action of the amphiphile AB . This is reflected not only in the increment of the mutual solubility of AA and BB , but also in providing a clear picture of the adsorption of the amphiphile at the liquid AA /liquid- BB interface (see Widom in Ref. 7). Also, the bulk phases exhibit micellar and bicontinuous structures that appear analogous to those of real surfactant solutions and microemulsions. The description of these structures is conveniently given by the already studied distribution of spin clusters in the equivalent Ising model (see Widom in Ref. 7).

All of these features are preserved in a straightforward manner when the model is extended to six components. There is, of course, an increment in the diversity of structures and configurations, and these in turn emerge in a much richer phase diagram that is now isomorphous to that of the FDG model. Provided the new "cosurfactant" species AC , BC , and CC only appear in small quantities, the WW2 model can be visualized as a perturbation to the original "oil" (AA), "water" (BB), and "surfactant" (AB) system. The effects of the additional degrees of freedom are remarkable; we have seen that there exist several phase progressions resembling those observed in real microemulsion systems, all requiring only a minority presence of the cosurfactants. These include three-liquid states terminating at different critical end points or at four-liquid states. The numerous cosurfactants appear also as convenient, and transparent (because of their symmetry) means of varying properties such as interfacial structure or curvature. The same effects are achieved in practice by changing the nature of the cosurfactant or through the addition of a salt to the aqueous phase. The WW2 model may prove to be a useful guide in the design of microemulsion systems by helping in the understanding of how global composition brings out, or suppresses, some phase properties of interest.

The existing isomorphism between the WW2 model and the FDG model suggests other applications when the main concern is the study of phase transitions and associated critical phenomena. The search of experimental evidence of some of the features of the global phase diagram of the FDG model, or of the closely related vdW mixture, is often hampered by the fact that the experimentalist can only observe a system phase diagram at a time. This is, of course, because the particle interactions are fixed when studying a particular ternary mixture. However, an ingenious method by means of which the experimentalist can alter the nature of the interactions is the consideration of the so-called quasibinary and quasiternary mixtures.^{15,16} Extra degrees of freedom can be added in a controlled manner when, in place of the three components, one uses a higher-component mixture where some of the constituent pairs of binary mixtures are chemically similar and completely miscible at the temperatures of interest.^{15,16}

The WW2 model provides a very different alternative in studying a global phase diagram. Here the strategy would be: Effectively replace the "interaction" fields by the chemical potential fields of the bifunctional components. The precise prescription given by Eqs. (5) and (6). In this way the entire global phase diagram can in

principle be sampled solely by means of composition manipulations. It is worth pointing out that certain features of the full phase diagram of the FDG model that appear artificial in terms of three (site) components accommodate as perfectly natural in the language of the WW2 model. An example is the symmetrical section in the large negative limit of $\bar{\mu}_{AB}$ (or large positive limit of the interaction parameter c). There it is necessary for some of the pair interparticle interactions to be highly repulsive at large separations.¹⁰ This region of the principal energy triangle only demands very low concentrations of the species AB in the WW2 version. And, as we have seen, the associated phase progressions, shown in Figs. 4, 7, and 8, resemble those observed experimentally in microemulsion systems,⁴⁻⁶ or those produced by calculations of their model counterparts.¹¹⁻¹³ The same limitation on the laboratory choices on the values of particle interactions in simple ternary systems (where no amphiphiles are present) would presumably preclude the observation of the features of the shield region in such systems.¹⁷ We have illustrated how the compressible version of the WW2 model with only three components incorporates the shield region in its phase diagram.

The Wheeler-Widom series of model mixtures do not

enjoy all the degrees of freedom one would consider these multicomponent systems would display. This is because the interactions amongst bifunctional molecules have been simplified to a minimum that only retains (through infinite repulsions or no interaction) the basic character of each constituent. Thus, in all of these models the temperature does not play a relevant role, and the ternary WW1 mixture only maps onto a one-component simple system, and the WW2 mixture onto a three-component incompressible fluid. It is therefore clear that the presence of multicritical points of high codimension in the full phase diagram of the FDG model, such as the δ , $\alpha\gamma$, and β^2 points, is perfectly natural in the WW2 language. The experimental evidence of the particular connectivity with which they appear in the diagram could be obtained through the examination of real amphiphile mixtures.

ACKNOWLEDGMENTS

We are grateful to E. Martina for valuable discussions. Financial support by Consejo Nacional de Ciencia y Tecnología de México is also acknowledged. One of us, A.R., would like to thank the John Simon Guggenheim Memorial Foundation for financial support.

-
- ¹K. Shinoda and H. Kuneida, *J. Colloid Interface Sci.* **42**, 381 (1973).
- ²I. Lo, F. Madsen, A. T. Florence, J. P. Treguier, M. Seiller, and F. Puisieux, in *Micellization, Solubilization, and Microemulsions*, edited by K. L. Mittal (Plenum, New York, 1977).
- ³P. G. de Gennes and C. Taupin, *J. Phys. Chem.* **86**, 2294 (1982).
- ⁴A. M. Bellocq, J. Biais, B. Clin, A. Gelot, P. Lalanne, and B. Lemanceau, *J. Colloid Interface Sci.* **74**, 311 (1980).
- ⁵A. M. Cazabat, D. Langevin, J. Meunier, and A. Pouchelon, *Adv. Colloid Interface Sci.* **16**, 175 (1982).
- ⁶K. E. Bennet, H. T. Davis, and L. E. Scriven, *J. Phys. Chem.* **86**, 3917 (1982).
- ⁷J. C. Wheeler and B. Widom, *J. Am. Chem. Soc.* **90**, 3064 (1968); B. Widom, *J. Phys. Chem.* **88**, 6508 (1984).
- ⁸D. Furman, S. Dattagupta, and R. B. Griffiths, *Phys. Rev. B* **15**, 441 (1977).
- ⁹R. L. Scott and P. H. van Konynenburg, *Discuss. Faraday Soc.* **49**, 87 (1970); P. H. van Konynenburg and R. L. Scott, *Philos. Trans. R. Soc. London Ser. A* **298**, 495 (1980).
- ¹⁰D. Furman and R. B. Griffiths, *Phys. Rev. A* **17**, 1139 (1978).
- ¹¹Y. Talmon and S. Prager, *Nature* **267**, 333 (1977).
- ¹²J. Jouffroy, P. Levinson and P. G. de Gennes, *J. Phys. (Paris)* **43**, 1241 (1982).
- ¹³B. Widom, *J. Chem. Phys.* **81**, 1030 (1984).
- ¹⁴J. Schulman and T. P. Hoar, *Nature* **152**, 102 (1943).
- ¹⁵B. K. Das and R. B. Griffiths, *J. Chem. Phys.* **70**, 5555 (1979).
- ¹⁶J. L. Creek, C. M. Knobler, and R. L. Scott, *J. Chem. Phys.* **74**, 3489 (1981); J. Specovious, M. A. Leiva, R. L. Scott, and C. M. Knobler, *J. Phys. Chem.* **85**, 2313 (1981); I. L. Pegg, *Kinam* **6A**, 3 (1984); and references therein.
- ¹⁷A region of four-phase points very probably belonging to a shield region has been observed experimentally in quaternary mixtures (see Ref. 15).